Regular Article

Check for
updates

Spatial patterns in a vegetation model with internal competition and feedback regulation

Salih Djilali[2,3,a], **Soufiane Bentout**[1,2,b], **Behzad Ghanbari**[4,5,c], **Sunil Kumar**[6,d]

[1] Department of Mathematics and Informatics, Center of Belhadj Bouchaib Ain Temouchent, BP 284 RP, 46000 Ain Temouchent, Algeria
[2] Laboratoire d'Analyse Non Linéaire et Mathématiques Appliquées. Département de Mathématiques, Université Abou Bakr Belkaïd, 13000 Tlemcen, Algeria
[3] Faculty of Exact sciences and informatics, Mathematic Department, Hassiba benbouali university, Chlef, Algeria
[4] Department of Engineering Science, Kermanshah University of Technology, Kermanshah, Iran
[5] Department of Mathematics, Faculty of Engineering and Natural Sciences, Bahçeşehir University, 34349 Istanbul, Turkey
[6] Department of Mathematics, National Institute of Technology, Jamshedpur, Jharkhand 831014, India

Abstract The vegetation patterns are a characteristic particularity of semiarid zones, which can be the future of modern ecology for its importance. This paper aims to study a diffusive vegetation model for the subject of studying the complex patterns generated by the presence of Turing-Hopf bifurcation. The main focus is on analyzing the effect of the locative internal rivalry between plants and feedback regulation on the pattern formations. The cross-diffusion produced by the positive feedback regulation generates surprising dynamics such as Hopf bifurcation, Turing bifurcation, Turing-Hopf bifurcation, which confirms the imbalance of the distribution of the vegetation in the semi-desert regions. For analyzing the spatiotemporal behavior near the Turing-Hopf bifurcation point, the Amplitude equation restricted at this point is used. Further, by using numerical simulations, the complex dynamics induced by the positive feedback redistribution and inner competition are explored.

1 Introduction

In the environment, the vegetation is widespread. This wealth is in huge danger due to the wide expansion of cities and the over carbon dioxide leak for a reason for our daily activities. The importance of the green cover is to suck the carbon dioxide and release the oxygen using what is known as photosynthesis, which is very important to our survival. For the safety of our planet, it must be a balance between the released carbon dioxide by different living beings and the sucked carbon by the plants by photosynthesis. Global warming and

[a] e-mails: djilali.salih@yahoo.fr; s.djilali@univ-chlef.dz

[b] e-mail: bentoutsofiane@gmail.com

[c] e-mail: b.ghanbary@yahoo.com

[d] e-mail: skumar.math@nitjsr.ac.in (corresponding author)

climate change are the direct consequence of the imbalance between releasing and suction of this toxic gas. At the moment, for the subject of reducing the concentration of this gas in the environmental air, the scientists tried to find a replacement of the lost green areas by the overbuilding of new cities. There is some work in augmenting the vegetation cover in different areas in the cities such as in the building (at the roof), gardens, shrubs, which is not enough. The semi-arid regions are the best places to begin. The main issue in these regions is the water, where the availability of this last is low. The quantity of water is crucial in determining the growth and expansion of the vegetation cover. This availability can be affected by many factors, and we mention rainfall, illumination, geographical conditions, graving. Consequently, various vegetation structures appear for different conditions, where this diversity is known by vegetation patterns [2,3,10–13]. In literature, there are numerous models that describe the relationship between water and plants. One of the first models is offered by Klausmerier [13], where the following spatiotemporal model is provided for modeling the connection between plant biomass (denoted by n) and water-limited biomass (denoted by w)

$$\begin{cases} \frac{\partial w}{\partial t} = R - w - wn^2 - \upsilon \frac{\partial w}{\partial x}, \\ \frac{\partial n}{\partial t} = wn^2 - \delta n + \Delta n. \end{cases} \tag{1.1}$$

R stands for the precipitation (soil, water) or rainfall rate; δ stands for the rate of natural death of plants; υ is the rate of the slope of terrain (or downhill runoff); the term wn^2 represents the amount of water absorbed by the plant or the long-range rivalry and short-range facilitation, Δ is the bidimensional Laplacian operator. It has been confirmed that this model predicts stripe patterns next to the wavelength which agrees with the real-life situation.

It is well known that the plants have the ability to redistribute the water in the soil. This point of view is used for the first time in water-plant interaction by Hardenberg et al. [35], where an expanded model is utilized for describing the feedback impact between vegetation biomass and water. The main idea is to add a cross-diffusion $\gamma\Delta(w - \beta n)$ in the water equation for modeling this feedback. The obtained system is:

$$\begin{cases} \frac{\partial w}{\partial t} = R - w - wn^2 - \upsilon \frac{\partial w}{\partial x} + \gamma\Delta(w - \beta n), \\ \frac{\partial n}{\partial t} = wn^2 - \delta n + \Delta n, \end{cases} \tag{1.2}$$

where γ is the rate corresponding to diffusion of the water in lack of vegetation. Using Darcy's law [35], we can model the transit of water through the soil. More precisely, the flux f is proportional to the water metric potential φ (which means that $fa - \nabla.\varphi$). The alternation of water due to the transit is $-\nabla.fa\nabla^2.\varphi$. By taking the following suction functional $\varphi = w - \beta n$ where w is the metric potential for the soil (see also [35]). In fact, the slope of terrain or the downhill runoff flow velocity is particular for some places not others, which means that it is not a necessary condition for having patterns. A numerical investigation is given for predicting wavelength, wave speed. Some works appear for describing the spatial patterns in the presence of cross-diffusion as [11,35]. Based on the best of our knowledge, the main mathematical achievement of these types of models is the dynamics introduced by Turing patterns. Further, for the subject of revealing the spatiotemporal patterns near Turing bifurcation point, where the amplitude equation restricted at Turing bifurcation point is used. The vegetation patterns was and still the subject of interest of many recent researches we mention as example the researches [1,5,6,18–21,27,33,34].

Very recently, the intensity of the inner competition reaction is considered in [37]. An extended model to Klausmeier's model (1.2) is considered. The investigated model is studied

in the following form:

$$\begin{cases} \frac{\partial w}{\partial t} = R - w - \frac{wn^2}{1+\tau n^2} - \upsilon \frac{\partial w}{\partial x}, \\ \frac{\partial n}{\partial t} = \frac{wn^2}{1+\tau n^2} - \delta n + \Delta n, \end{cases} \tag{1.3}$$

where the numerator in the term $\frac{wn^2}{1+\tau n^2}$ is the water absorbed by a plant as it has been highlighted in the above model (1.1), and the dominator as inner (or local) competition between biomass. The main idea in considering this term is due to the gathering of water by plants using preferential leaking in the vegetated zone and run-on/run-off from desert regions toward grassed ones. The intensity of competition increases for the densely vegetated areas. The issue of the previous competition functional is the unboundedness of this last for the densely vegetated area which is not true mostly for the semi-deserts areas, where the available water for each unit of the biomass of plants may reduce if the inner rivalry induced negative feedback is more intense, then the leaking induces positive feedback. To mention that in [37], it has been proved that the system (1.3) cannot undergo Turing patterns. Indeed, we consider in this paper the presence of the cross-diffusion in the system (1.3) subjects to the homogeneous no-flux boundary conditions, which means that

$$\begin{cases} \frac{\partial w}{\partial t} = R - w - \frac{wn^2}{1+\tau n^2} - \upsilon \frac{\partial w}{\partial X} + \gamma \Delta(w - \beta n), \quad X \in \Omega, t > 0, \\ \frac{\partial n}{\partial t} = \frac{wn^2}{1+\tau n^2} - \delta n + \Delta n, \quad X \in \Omega, t > 0, \\ \frac{\partial w}{\partial \mathbf{v}} = \frac{\partial n}{\partial \mathbf{v}} = 0, \quad X \in \Omega, t > 0, \\ w(X, 0) = w_0(X) \geq 0, n(X, 0) = n_0(X) \geq 0 \quad X \in \Omega, \end{cases} \tag{1.4}$$

where Ω is assumed to be a bounded set of $\mathbb{R}^2$ with a smooth boundary. The importance of considering such a model is for generalizing the previous models where the model (1.4) considers various factors such as feedback regulation, water redistribution, the intensity of inner rivalry where each one of the previous models lacks these components (partially or entirely). More precisely, the system (1.2) can be considered as a special case of the system (1.4), wherein the absence of cross-diffusion (means that $\gamma = 0$ the system becomes the system (1.3). Moreover, in the absence of the inner competition of plants, the system returns to the model (1.2). For the nonexistence on both the inner rivalry of plants and the feedback regulation, the system (1.4) becomes system (1.1), which shows the richness of this system. Further, in the absence of slope of downhill (means that $\upsilon = 0$) the system can imply many works. For further discussions we rewrite the system (1.3) in the absence of the slope of terrain in the following form:

$$\begin{cases} \frac{\partial w}{\partial t} = R - w - \frac{wn^2}{1+\tau n^2} + \gamma \Delta(w - \beta n), \quad X = (x, y) \in \Omega, t > 0, \\ \frac{\partial n}{\partial t} = \frac{wn^2}{1+\tau n^2} - \delta n + \Delta n, \quad X = (x, y) \in \Omega, t > 0, \\ \frac{\partial w}{\partial \mathbf{v}} = \frac{\partial n}{\partial \mathbf{v}} = 0, \quad X = (x, y) \in \Omega, t > 0, \\ w(x, y, 0) = w_0(x, y) \geq 0, n(x, y, 0) = n_0(x, y) \geq 0. \end{cases} \tag{1.5}$$

As it has been previously mentioned that the system (1.5) implies many recent works, such as the case of the absence of inner rivalry $\tau = 0$ is discussed in [11], where the existence of Turing patterns, and for discussing the spatiotemporal patterns near the Turing bifurcation points the Amplitude equation is used. Ref. [36] discusses the pattern formations in detail.

Indeed, it is proved in [37] that the system (1.3) has no Turing bifurcation. Consequently, the main focus was on studying the effect of the impact of the slop of terrain and the internal competition between the plants on the vegetation patterns. Here, we will focus on studying the impact of cross-diffusion in the water equation which is generated by taking into consideration

the redistribution of the water in the soil next to the internal competition between the plants on the vegetation spatial patterns. Recently, it has been confirmed by [11] that this cross-diffusion generates Turing patterns for the model (1.2) (which is a particular case of our model $\tau = 0$). Turing patterns have the responsibility for determining the complex pattern that we can get in the real world. On the other hand, The Hopf bifurcation is also very important for determining the existence of the periodic solutions for the spatial systems where the presence of periodic orbits can explain the seasonality of the vegetation grows, which agrees with the real-world situation. To mention that the spatial Hopf bifurcation has never been proved for the vegetation model, and no one can deny its importance in predicting the vegetation patterns. Further, the present paper is not restricted to proving these kinds of patterns. Our main objective is to determine the patterns generated by the intermingling of Turing and Hopf bifurcations, which known as Turing-Hopf bifurcation. To highlight that Turing-Hopf bifurcation is recently investigated which elaborated by the intermingling of both Hopf and Turing bifurcation for different values of wavenumber, we refer as an example the papers [4,9,14,29–31]. Turing–Hopf bifurcation has never been studied for vegetation models. Indeed, it has been ensured by many researchers that this kind of bifurcation generates very complex dynamics. To the best of our knowledge the existence of Turing–Hopf bifurcation is confined in one-dimensional space. Thus, our second perspective is to prove the existence of this kind of co-dimensional bifurcation in the case of two-dimensional spatial variables. In literature, for analyzing the spatiotemporal behavior near the Turing-Hopf bifurcation, the normal form on the center of the manifold [31] is always considered. In this paper, by using the Amplitude equations restricted at the Turing-Hopf bifurcation point, is used. Also to mention there are a few works that deal with the effect of cross-diffusion (positive constants of cross-diffusion) on the value of Turing-Hopf bifurcation. But in this paper, we consider another kind of cross-diffusions (negative cross-diffusion $\gamma \beta \Delta n$). The Turing-Hopf bifurcation can generate important patterns that consist of a different distribution of the water and the vegetation cover which agrees with the real-life situation. Periodic solutions can model the seasonality of vegetation growth. Studying the vegetation model (1.5) can help the scientists to determine the right condition for the evolution of the vegetation cover mostly in desert and semi-desert areas. Besides, Determining global behavior as example [38–46] and local behavior [7,8,22–26,28] is very important to anticipate the biological evolution of the species the the degree of the spread of infectious diseases, where it provides some the time and appropriate (or optimal) suggestion for having the best result (as avoiding the extinction of species, and guaranteeing the stop of the spread of some infectious diseases for epidemiological perspectives). For the ecological and the mathematical perspective, we organize the paper in the following manner:

- In the next section, the well-posedness of the problem is proved using the theory of invariant regions.
- Section three is the main part of the paper, where some results are proved for the first time for the vegetation models. In fact, the dynamics introduced in the absence of diffusion where the existence of Hopf bifurcation is proved (actually, the authors in [37] do not deal with a possible bifurcation that the system can undergo) this result is expanded in the presence of diffusion where the rainfall rate is used as a bifurcation parameter. The existence of Turing bifurcation is proved under some appropriate conditions on the model's parameters. Further, the existence of Turing-Hopf bifurcation is also investigated next to its effect on the spatiotemporal patterns of the solution where the amplitude equations are used to determine these complex patterns.
- A numerical simulation section is offered to emphasize the obtained theoretical results and shows the complex dynamics generated by the presence of Turing-Hopf bifurcation.

- A final discussion and remarks conclude the paper.

2 Existence, positivity of solution

In this section, we shall prove the existence of positive solution for the system (1.5), where the result is resumed in the following theorem:

Theorem 2.1 *Assume that $w_0(x, y) \geq 0$ and $n_0(x, y) \geq 0$ then the system (1.5) has a unique positive solution.*

Proof By putting

$$f_1(w, n) = R - w - \frac{wn^2}{1 + \tau n^2}, \text{ and } f_2(w, n) = \frac{wn^2}{1 + \tau n^2} - \delta n,$$

and the linear operator

$$\Lambda = \begin{pmatrix} \Delta & 0 \\ 0 & \Delta \end{pmatrix},$$

The system (1.5) can be rewritten in the following structure

$$\frac{dU}{dt} = D\Lambda U + F(U), \tag{2.1}$$

where

$$D = \begin{pmatrix} \gamma & -\gamma\beta \\ 0 & 1 \end{pmatrix}, \quad \text{and} \quad F = \begin{pmatrix} f_1 \\ f_2 \end{pmatrix},$$

It remains to determine the space at which the linear operator Λ generates a C_0 semi–group, the appropriate space is $\left(H^1(\mathbb{R}^2)\right)^2$ (which means that $H^1(\mathbb{R}^2) \times H^1(\mathbb{R}^2)$). Under the norm $\|U\| = \left(\int_{\mathbb{R}^2} \left(|w|^2 + |\nabla w|^2 + |n|^2 + |\nabla n|^2\right) dX\right)^{\frac{1}{2}}$, where $X = (x, y)^T \in \mathbb{R}^2$ the completion of the space $\left(C_0^\infty(\mathbb{R}^2)\right)^2$ is $\left(H^1(\mathbb{R}^2)\right)^2$ where the linear operation is well defined in this space.

Defining $\Lambda U = (\triangle w, \triangle n)$ where $U = (w, n) \in D(\Lambda) := \left(H^1(\mathbb{R}^2)\right)^2$, which means that Λ generates a C_0 semigroup. Now let us focus on verifying that $f_i, i = 1, 2$ are a Lipschitz functionals. By putting

$$|f_1(w_1, n_1) - f_1(w_2, n_2)| = \left| -w_1 - \frac{w_1 n_1^2}{1 + \tau n_1^2} + w_2 + \frac{w_2 n_2^2}{1 + \tau n_2^2} \right|,$$

we get

$$\leq |w_1 - w_2| + \left| \frac{w_1 n_1^2}{1 + \tau n_1^2} - \frac{w_2 n_2^2}{1 + \tau n_2^2} \right|,$$

$$\leq |w_1 - w_2| + \frac{M^2}{1 + \tau M^2}(|w_1 - w_2| + |n_1 - n_2|),$$

$$\leq \frac{1 + (1 + \tau)M^2}{1 + \tau M^2}|w_1 - w_2| + \frac{M^2}{1 + \tau M^2}|n_1 - n_2|,$$

Hence, f_1 is suitably Lipschitz, By the same manner we have

$$|f_2(w_1, n_1) - f_2(w_2, n_2)| = \left| \frac{w_1 n_1^2}{1 + \tau n_1^2} - \delta n_1 - \frac{w_2 n_2^2}{1 + \tau n_2^2} + \delta n_2 \right|,$$

which leads to

$$\leq \delta|n_1 - n_2| + \left| \frac{w_1 n_1^2}{1 + \tau n_1^2} - \frac{w_2 n_2^2}{1 + \tau n_2^2} \right|,$$

$$\leq |w_1 - w_2| + \frac{M^2}{1 + \tau M^2}(|w_1 - w_2| + |n_1 - n_2|),$$

$$\leq \frac{1 + (1 + \tau)M^2}{1 + \tau M^2}|n_1 - n_2| + \frac{M^2}{1 + \tau M^2}|w_1 - w_2|,$$

which means that f_2 is also suitably Lipschitz. It is not though to check that

$$|F(w_1, n_1) - F(w_2, n_2)| \leq \left(\frac{1 + (1 + \tau)M^2}{1 + \tau M^2} + \frac{M^2}{1 + \tau M^2} \right)|w_1 - w_2|$$

$$+ \left(\frac{1 + (1 + \tau)M^2}{1 + \tau M^2} + \frac{M^2}{1 + \tau M^2} \right)|n_1 - n_2|$$

thus

$$|F(w_1, n_1) - F(w_2, n_2)| \leq \frac{1 + (2 + \tau)M^2}{1 + \tau M^2}(|w_1 - w_2| + |n_1 - n_2|).$$

Using the standard theory of C_0 semi group (see [17]) we deduce the existence and the uniqueness of a positive solution. Here we considered the positivity and the boundedness of solution where a common bound denoted by M is used for simplifying the computations. The proof is completed. □

3 Complex spatiotemporal patterns generated by taking into consideration of the plant's effect on the redistribution of the water in the soil

3.1 Linear analysis: Hopf, Turing, Turing-Hopf bifurcations

This section demonstrates the existence of the Turing-Hopf bifurcation. First of all, the system (1.5) has the following homogeneous steady states

- $E_0 = (R, 0)$ which models the desert state.
- $E_\pm = (w_\pm, n_\pm)$ which models the coexistence of both water and vegetation biomass, where

$$w_\pm = \frac{\delta(1 + \tau n_\pm^2)}{n_\pm} \quad \text{and} \quad n_\pm = \frac{1}{2\delta(1 + \tau)}\left(R \pm \sqrt{R^2 - 4(1 + \tau)\delta^2} \right),$$

which has its biological significant if and only if $R > R_{\min} := 2\delta\sqrt{1 + \tau}$

For determining the local stability of the vegetation steady states $E_\pm$ we use the translation to the origin in the form

$$V(t) = \begin{pmatrix} \tilde{w} \\ \tilde{n} \end{pmatrix} = \begin{pmatrix} w - w_\pm \\ n - n_\pm \end{pmatrix},$$

Neglecting the tilde for simplicity, the system (1.5) can be expressed in the following manner:

$$V_t = J_\pm \begin{pmatrix} w \\ n \end{pmatrix} + \begin{pmatrix} f_1(w, n) \\ f_2(w, n) \end{pmatrix} + D\triangle V, \tag{3.1}$$

where Vt is the partial derivative of V with respect to t and $J_\pm$ is the Jacobian matrix of the system (1.5) in the absence of diffusion at the vegetation equilibrium state $E_\pm$ which is given

as follows:

$$J_\pm = \begin{pmatrix} -\frac{n_\pm^2}{1+\tau n_\pm^2} - 1 & \frac{-2\delta}{1+\tau n_\pm^2} \\ \frac{n_\pm^2}{1+\tau n_\pm^2} & \frac{2\delta}{1+\tau n_\pm^2} - \delta \end{pmatrix}, \tag{3.2}$$

we put

$$\alpha_{11} = -\frac{1+(1+\tau)n_+^2}{1+\tau n_+^2} \quad \alpha_{12} = \frac{-2\delta}{1+\tau n_+^2}$$
$$\alpha_{21} = \frac{n_+^2}{1+\tau n_+^2} \quad \alpha_{22} = \frac{\delta - \delta\tau n_+^2}{1+\tau n_+^2}$$

and

$$f_1(w, n) = \alpha_1 w^2 + \alpha_2 wn + \alpha_3 n^2 + \alpha_4 w^3 + \cdots,$$
$$f_2(w, n) = \beta_1 w^2 + \beta_2 wn + \beta_3 n^2 + \beta_4 n^3 + \cdots,$$
$$\alpha_1 = 0 \qquad \beta_1 = 0$$
$$\alpha_2 = \frac{-2n_+}{(1+\tau n_+^2)^2} \qquad \beta_2 = \frac{2n_+}{(1+\tau n_+^2)^2},$$
$$\alpha_3 = \frac{-4n_+(1-\tau n_+^2)}{(1+\tau n_+^2)^2} \quad \beta_3 = \frac{2w(1-2\tau n_+^2)}{(1+\tau n_+^2)^3},$$
$$\alpha_4 = 0 \qquad \beta_4 = 0.$$

The linearized system of (3.1) at an arbitrary homogeneous steady state is expressed as follows:

$$V_t = J_\pm \begin{pmatrix} w \\ n \end{pmatrix} + D \begin{pmatrix} \triangle w \\ \triangle n \end{pmatrix}. \tag{3.3}$$

The linear stability of the vegetation homogeneous steady states $E_\pm$ implies that the system (3.3) admits the following solution

$$\begin{pmatrix} w \\ n \end{pmatrix} = \begin{pmatrix} c_1 \\ c_2 \end{pmatrix} exp(\lambda t + i\upsilon \cdot x).$$

The characteristic equation associated with the above equation (3.3) is given as:

$$\Psi_\upsilon \triangleq \lambda^2 - T_\upsilon \lambda + D_\upsilon = 0, \ \upsilon \in \mathbb{N}_0, \tag{3.4}$$

where

$$T_\upsilon = \frac{\delta - 1 - (1+\tau+\delta\tau)n_\pm^2}{1+\tau n_\pm^2} - (\gamma+1)\upsilon^2,$$
$$D_\upsilon = \gamma\upsilon^4 + \upsilon^2 \left(\frac{-(1+(1+\tau)n_\pm^2)+\gamma(\delta+(\beta-\tau)n_\pm^2)}{1+\tau n_\pm^2} \right) + \frac{\delta(1+\tau)\left(n_\pm^2 - \frac{1}{1+\tau}\right)}{1+\tau n_\pm^2}. \tag{3.5}$$

The roots of the characteristic Eq. (3.4) can be found as:

$$\lambda_\upsilon = \frac{1}{2}\left(T_\upsilon \pm \sqrt{T_\upsilon^2 - 4D_\upsilon} \right),$$

In order to set the stability conditions generated by the absence of cross-diffusion we consider the following theorem

Theorem 3.1 (Dynamics introduced by the absence of diffusion) *Assume that $R > R_{\min}$ holds, the system (1.5) in the case of absence of diffusion (means that $\upsilon = 0$) verifies the following aspects*

(i) *The equilibrium state E_- is unconditionally unstable.*

(ii) *For $\delta < 1$ then E_+ is unconditionally stable.*

(iii) *The equilibrium state E_+ is stable for ($\delta > 1$ and $R > R_{H,0+} := \delta(1+\tau)\sqrt{\frac{\delta-1}{1+\tau+\delta\tau}}$) and unstable for ($\delta > 1$ and $R < R_{H,0+}$)*

(iv) *For $\upsilon = 0$ (or in the absence of diffusion) next to the condition $\delta > 1$ the system (1.5) undergoes Hopf bifurcation at $R = R_{H,0+}$.*

Proof Putting $n = 0$ in D_n defined in (3.5), we obtain:

$$D_0 = \frac{\delta(1+\tau)\left(n_{\pm}^2 - \frac{1}{1+\tau}\right)}{1+\tau n_{\pm}^2}, \tag{3.6}$$

and by doing some formal calculations, we have:

$$n_- - \frac{1}{\sqrt{1+\tau}} = \frac{-2(R - 2\delta\sqrt{1+\tau})}{\sqrt{1+\tau}\left(R - 2\delta\sqrt{1+\tau} + \sqrt{R^2 - 4\delta^2(1+\tau)}\right)} < 0.$$

The last result leads to deduce that $D_0 < 0$ for $R > R_{\min}$, which means that the homogenous steady-state (w_-, n_-) is saddle. Hence, it is unstable. Thus (i) holds. Besides,

$$n_+ - \frac{1}{\sqrt{1+\tau}} = \frac{(R - 2\delta\sqrt{1+\tau})(R + 2\delta\sqrt{1+\tau}) + \sqrt{R^2 - 4\delta^2(1+\tau)}}{\left(R + \sqrt{R^2 - 4\delta^2(1+\tau)} + \sqrt{1+\tau}\right)\delta(1+\tau)} > 0.$$

Thus, $D_0 > 0$ under the condition $R > R_{\min}$, this, takes us to deduce that T_0 determines the stability of the equilibrium E_+ in the absence of cross-diffusion. For $n = 0$ the sign of T_0 determines the local behavior of the equilibrium state E_+. In other words, $T_0 < 0$ holds if and only if

$$\delta > 1 + (1 + \tau + \delta\tau)n_+^2. \tag{3.7}$$

It is easy to verify that for $\delta < 1$ one has $T_0 < 0$; which means that E_+ is locally stable under this condition (then (ii) is checked). Now focusing on studying the local behavior offered by the condition $\delta > 1$ and $R > R_{\min}$. Under these conditions the inequality (3.7) becomes:

$$R > R_{H,0}^+ := \sqrt{\frac{\delta^2(\delta-1)(1+\tau)^2}{1+\tau+\delta\tau}} + \sqrt{\frac{\delta^2(1+\tau+\delta\tau)}{\delta-1}}. \tag{3.8}$$

It is easy to see that under the condition $\delta > 1$, E_+ is stable for $R > R_{H,0}^+$ and unstable for $R < R_{H,0}^+$. Further, for $R = R_{H,0}^+$ the characteristic equation has two purely imaginary roots $\pm\sqrt{\frac{\delta(1+\tau)\left(n_+^2 - \frac{1}{1+\delta}\right)}{1+\tau n_+^2}}$ which means that for showing the existence of Hopf bifurcation it remains to verify the transversality condition which is given as follows:

$$\frac{d\Re(\lambda)}{dR}\bigg|_{R=R_{H,0}^+} = n_+(2 - \delta + (1+\tau)(1+\delta)n_+^2)\frac{dn_+}{dR}\bigg|_{R=R_{H,0}^+}.$$

By using the fact that $n_+ > \frac{1}{\sqrt{1+\tau}}$ leads to deduce that $2 - \delta + (1+\tau)(1+\delta)n_+^2 > 3 > 0$. Further

$$\left.\frac{dn_+}{dR}\right|_{R=R_{H,0}^+} = \frac{1}{2\delta(1+\tau)}\left(1 + \frac{2R_{H,0}^+}{2\sqrt{\left(R_{H,0}^+\right)^2 + 4\delta^2(1+\tau)}}\right) > 0.$$

Combining the two results, we deduce that $\left.\frac{d\Re(\lambda)}{dR}\right|_{R=R_{H,0}^+} > 0$ which means that the system (1.5) undertakes Hopf bifurcation for $n = 0$ at $R = R_{H,0}^+$. This puts an end to the proof. □

It has been confirmed by Turing [32] that diffusion can lead to instability where for some values of the diffusion parameters, we can have instability, such as instability is called by diffusion-driven instability or by Turing instability. In fact, this kind of instability appears when the following conditions hold true:

$$\Im\lambda_\upsilon \neq 0, \Re\lambda_\upsilon = 0, k = k_T \neq 0.$$

where $\Re$ and $\Im$ stand for the real part and the imaginary part functionals, respectively. It is not tough to prove that the following equation is a sufficient condition for having Turing bifurcation:

$$\delta - 1 - (1+\tau+\delta\tau)n_+^2 + \sqrt{\frac{|\delta - 1 - (1+\tau+\delta\tau)n_+^2|}{\gamma(1+\delta n_+^2)}}\left[(1+\tau)n_+^2 + 1 + 2\gamma\beta\delta + 2\gamma\delta\tau n_+^2\right]$$
$$+\delta(1+\tau)\left(n_+^2 - \frac{1}{1+\tau}\right) = 0.$$

For the existence of Hopf bifurcation for the spatiotemporal vegetation model (1.5) we set the following theorem.

Theorem 3.2 (The existence of Hopf bifurcation for the spatial system) *Assume that $R > R_{\min}$, then the following results arises.*

(i) *The system (1.5) cannot undergo Hopf bifurcation at E_-.*
(ii) *For $\delta < 1$: The system (1.5) cannot undergo Hopf bifurcation at the constant steady state E_+.*
(iii) *For $\delta > 1$: There exists a wave number denoted by $\vartheta_H \geq 0$ such that system (1.5) undertakes Hopf bifurcation for the constant steady state E_+ at $R = R_{\vartheta,H}$, where this homogeneous steady state is locally stable for $R > \max\{R_{0,H}, R_{\min}\}$ and unstable for $R_{\min} < R < R_{0,H}$. Further, a spatially homogeneous periodic solution appears for $\vartheta = 0$ and nonhomogeneous ones appear for $\vartheta = 1, 2, \ldots, \vartheta_H$.*

Proof It has been proved in Theorem 2.1 that $D_0 < 0$ for the equilibrium E_- which leads to deduce that there exists a positive integer (wavenumber) verifying $D_\vartheta < 0$ ($\vartheta = 0$) which leads to claim that this homogeneous steady state stays unstable in the presence of the diffusion which confirms the obtained result in (i).

Passing to the second part of the proof. It is easy to see that the condition $T_\vartheta = 0$ is an indispensable but not enough condition for getting Hopf bifurcation. Obviously, by taking a look at (3.5) we can deduce that under $\delta < 1$ we get $T_\vartheta < 0$, which leads us to deduce that the system (1.5) cannot possess Hof bifurcation at the equilibrium E_+, which emphasizes (ii).

Now, it remains the main part of the proof, where we will proceed to show the existence of Hopf bifurcation. In addition to the main assumption $R > R_{min}$, we suppose that $\delta > 1$. In what follows, we choose the rainfall constant as a bifurcation parameter. It is well known that Hopf bifurcation occurs if the characteristic equation (3.4) has purely imaginary roots in addition to the transversality condition, which equivalent to

$$T_\vartheta = 0, \ D_\vartheta \neq 0, \quad \left.\frac{d\Re(\lambda)}{dR}\right|_{R=R_{\vartheta,H}} \neq 0.$$

$T_\vartheta = 0$ is equivalent to

$$n_+^2 = \frac{\delta - 1 - (\gamma + 1)\vartheta^2}{1 + \tau + \delta\tau + (\gamma + 1)\tau\vartheta^2}, \tag{3.9}$$

using the fact that $\delta > 1$ we can make sure that the critical wave numbers such that the system (1.5) could possess Hopf bifurcation are $\vartheta = 0, 1, ..., \vartheta_c$ where

$$\vartheta_c := \max \{\vartheta \in \mathbb{N}, \ \delta - 1 - (\gamma + 1)\vartheta^2 > 0\} := \left[\sqrt{\frac{\delta - 1}{\gamma + 1}}\right],$$

where [.] represents the integer part function. Now, considering the wave number be part of the set $\{0, 1, ..., \vartheta_c\}$ and making use of the explicit formula of n_+, (3.9) becomes

$$R + \sqrt{R^2 - 4\delta^2(\tau + 1)} = 2\delta(1 + \tau)\sqrt{\frac{\delta - 1 - (\gamma + 1)\vartheta^2}{1 + \tau + \tau\delta + \tau\vartheta^2(\gamma + 1)}},$$

This equivalent to

$$R = R_{\vartheta,H} := \delta\frac{(\delta - 1 - (\gamma + 1)\vartheta^2) + 1 + 2\delta\tau}{\sqrt{(\delta - 1 - (\gamma + 1)\vartheta^2)(1 + \tau + \delta\tau + (\gamma + 1)\vartheta^2)}} > 0,$$

$$\text{for } \vartheta = 0, 1, ..., \vartheta_c, \delta < 1.$$

For having purely imaginary roots, we must have $D_\vartheta > 0$, it is easy to see that $D_0 > 0$ which means that there exist a wave numbers $\vartheta_{c_2} > 0$ such that $D_\vartheta > 0$ for $\vartheta \in \{0, 1, ..., \vartheta_{c_2}\}$. In fact, by considering $\vartheta_H = \min\{\vartheta_c, \vartheta_{c_2}\}$ we can claim that the characteristic equation (3.4) has a purely imaginary roots $\pm\sqrt{D_\vartheta}$ where $\vartheta = \{0, 1, ..., \vartheta_H\}$. Now it remains to confirm the transversality condition which is given in the following form

$$\left.\frac{d\Re}{dR}\right|_{R=R_{H,\vartheta}} = \frac{n_{+,H}(2 - \delta + (1 + \tau)(1 + \delta)n_{+,H}^2)}{2\delta(1 + \tau)}\left(1 + \frac{2R_{H,\vartheta}^+}{2\sqrt{\left(R_{H,\vartheta}^+\right)^2 + 4\delta^2(1 + \tau)}}\right) > 0,$$

where $n_{+,H} = \frac{R_{H,\vartheta} + \sqrt{R_{H,\vartheta}^2 - 4\delta^2(\tau+1)}}{2\delta(1+\tau)}$, $\vartheta = 0, 1, ..., \vartheta_H$. The proof is successfully established.   □

Now let us focus on studying the existence of Turing-Hopf bifurcation. From many papers such as [4,9,14,29–31] we can confirm that Turing-Hopf bifurcation appears at a reaction-diffusion system if there exist two different wavenumbers denoted by ϑ_H and $\vartheta_T \neq 0$ where the vegetation system (1.5) undergoes Hopf bifurcation at $\vartheta = \vartheta_H$ and undergoes Turing bifurcation at $\vartheta = \vartheta_T$, and the transversality condition holds. It has been proved widely that this kind of bifurcation affects the spatiotemporal behavior of the solution which is going to

anticipate this kind of complex dynamics. Indeed, by taking into consideration the results presented in Theorem 3.1, we can conclude that the system (1.5) undertakes Hopf bifurcation at $R = R_{0,H}$ for the equilibrium state E_+, we denote by L_H for Hopf bifurcation curve on $R - \gamma$ plan. In other words, the system (1.5) has Hopf bifurcation for $\vartheta = \vartheta_H = 0$ for the vegetation homogeneous steady state E_+. Now it remains to show the existence of a strictly positive wave number denoted by ϑ_T such that the system undergoes Turing bifurcation at different bifurcation parameters than the rainfall rate. In fact, we will choose the diffusion rate of the water biomass γ as a bifurcation parameter. Also, we consider the $R - \gamma$ plan. Solving $D_\vartheta = 0$ in γ we get:

$$\gamma_T(\vartheta) = \frac{\delta(1+\tau)\left(n_+^2 - \frac{1}{1+\tau}\right) + ((1+\tau)n_+^2 + 1)\vartheta^2}{\vartheta^2\left(-(1+\tau n_+^2)\vartheta^2 + \delta + n_+^2(\beta - \delta\tau)\right)}, \tag{3.10}$$

where n_+ restricted at $R_{H,0}$ which means that

$$n_+|_{R=R_{H,0}} := \frac{1}{2\delta(1+\tau)}\left(R_{H,0} + \sqrt{R_{H,0}^2 - 4(1+\tau)\delta^2}\right),$$

and $\vartheta \in \{1, 2, ..., \vartheta^*\}$ where

$$\vartheta^* := \left[\sqrt{\frac{\delta + n_+^2(\beta - \delta\tau)}{1 + \tau n_+^2}}\right]$$

and $\beta > \beta_{min} := \max\left\{0, \frac{\delta(1-\tau n_+^2)}{n_+^2}\right\}$. Setting the positive real x where $1 \leqslant x \leqslant \vartheta^*$. The differentiation of the functional $\gamma_T(x)$ with respect to x is given as

$$\gamma_T'(x) = \frac{(1+(1+\tau)n_+^2)x^2 + 2\delta((1+\tau)n_+^2 - 1)x - \frac{\delta((1+\tau)n_+^2 - 1)(\delta + n_+^2(\beta - \delta\tau))}{1+\tau n_+^2}}{x^2\left(-(1+\tau n_+^2)x + \frac{\delta + n_+^2(\beta - \delta\tau)}{1+\tau n_+^2}\right)^2}.$$

In fact, the sign of $\gamma'(x)$ is given as follows

$$\gamma_T'(x) = \begin{cases} > 0 & \text{for } x > x^*, \\ < 0 & \text{for } x < x^*, \end{cases}$$

where

$$x^* = \frac{1}{1+(1+\tau)n_+^2}\left\{\delta((1+\tau)n_+^2 - 1) + \sqrt{\frac{\delta((1+\tau)n_+^2 - 1)n_+^2}{1 + \tau n_+^2}(2\delta + 1 + (1+\tau)n_+^2)}\right\}.$$

This result means that the functional γ reaches its maximum either at 1 or ϑ^{*^2} which allows us to set the following integer:

$$\vartheta_T = \begin{cases} 1 & \text{if } \gamma_T(1) > \gamma_T(\vartheta^{*^2}), \\ \vartheta^* & \text{if } \gamma_T(1) < \gamma_T(\vartheta^{*^2}). \end{cases}$$

We proved that there exists a positive intersection point between the Hopf bifurcation curve defined by $R = R_{0,H}$ in $R - \gamma$ plan (curve L_H in Fig. 4) and the Turing bifurcation curve defined by $\gamma = \gamma_T(\vartheta^2)$ (L_T in in Fig. 4). Then we have

$$\frac{d\Re\lambda(R)}{dR}\bigg|_{R=R_{H,0}} = \frac{n_{+,H}(2 - \delta + (1 + \tau)(1 + \delta)n_{+,H}^2)}{2\delta(1 + \tau)}\left(1 + \frac{2R_{H,0}}{2\sqrt{\left(R_{H,0}\right)^2 + 4\delta^2(1 + \tau)}}\right) > 0.$$

where $n_{+,H} = \frac{R_{H,0} + \sqrt{R_{H,0}^2 - 4\delta^2(\tau+1)}}{2\delta(1+\tau)}$, and also we have

$$\frac{d\Re\lambda(R)}{dR}\bigg|_{L_T} = \frac{2n_+}{(1 + \tau n_+)^2 T_\vartheta}\left[\vartheta^2(-1 + \gamma(\beta + \tau - \delta\tau)) + \delta(1 + 2\tau)\right]\frac{dn_+}{dR}\bigg|_{L_T} \neq 0.$$

The obtained results are summarized in the following theorem:

Theorem 3.3 *Assume that $R > R_{\min}$ an $\delta > 1$ then we have:*

The Hopf bifurcation curve L_H (corresponding the wavenumber 0) intersects the Turing bifurcation curve L_T and a codimension-2 Turing–Hopf bifurcation occurs at the intersect point $(R_{0,H}, \gamma_T(\vartheta_T))$, where

$$\gamma_T(\vartheta_T) = \frac{\delta(1 + \tau)\left(n_+^2 - \frac{1}{1+\tau}\right) + ((1 + \tau)n_+^2 + 1)\vartheta_T^2}{\vartheta_T^2\left(-(1 + \tau n_+^2)\vartheta_T^2 + \delta + n_+^2(\beta - \delta\tau)\right)},$$

and

$$\vartheta_T = \begin{cases} 1 & \text{if } \gamma_T(1) > \gamma_T(\vartheta^{*2}), \\ \vartheta^* & \text{if } \gamma_T(1) < \gamma_T(\vartheta^{*2}). \end{cases}$$

and

$$R > R_{H,0+} := \delta(1 + \tau)\sqrt{\frac{\delta - 1}{1 + \tau + \delta\tau}}$$

Further, for $(R, \gamma) = (R_{0,H}, \gamma_T(\vartheta_T))$ the characteristic equation Ψ_0 has a pair of purely imaginary roots $\pm i\omega_c$ and Ψ_{ϑ_T} has a simple zero root, and for (3.4), there are no other roots with zero real part.

3.2 Nonlinear analysis: The spatiotemporal patterns generated by the presence of Turing-Hopf bifurcation

In this subsection, we will derive the amplitude equations restricted at the Turing-Hopf bifurcation point with the help of the weakly nonlinear analysis. The main interest in considering it is to analyze the complex dynamics next to the Turing-Hopf bifurcation. In fact, the Turing mode $T(\vartheta_T, 0)$ where ϑ_T is the wavenumber will interact with the Hopf bifurcation mode (homogeneous) denoted by $H(0, \omega_H)$ where ω_H is the frequency. The solution of the system (1.5) can be expressed in the following manner:

$$U = \varepsilon U^{(1)} + \varepsilon^2 U^{(2)} + \varepsilon^3 U^{(3)} + \cdots, \tag{3.11}$$

where

$$U^{(1)} = \Sigma_\nu[A_\nu \exp^{(i\vartheta_j.x)} + B \exp^{(i\omega_H t)}] + c.c.,$$

where $c.c.$ stands for the conjugate term. By letting $\kappa = \upsilon^2 t$ be the slow time and expands w and n. The bifurcation parameters are R and γ, then

$$
\begin{aligned}
&\binom{w}{n} = \varepsilon\binom{w_1}{n_1} + \varepsilon^2\binom{w_2}{n_2} + \varepsilon^3\binom{w_3}{n_3} + \cdots \\
&R = R_{H,0} + R^{(2)}\upsilon^2. \\
&\gamma = \gamma_T^* + \gamma^{(2)}\upsilon^2.
\end{aligned}
\tag{3.12}
$$

Suppose that the amplitude Λ_j and the Hopf mode Φ are lingeringly changing variable, this means:

$$
\begin{aligned}
\frac{d\Lambda_j}{dt} &= \varepsilon^2\frac{d\Lambda_j}{d\kappa} + O(\varepsilon^2), \\
\frac{d\Phi}{dt} &= \varepsilon^2\frac{d\Phi}{d\kappa} + O(\varepsilon^2).
\end{aligned}
$$

Using (3.12) into the system (3.3), and gathering the first and the second the third power of ε, the sequence of equations can be expressed in the following manner

$$
\begin{aligned}
O(\varepsilon) &: M_\vartheta\binom{w_1}{n_1} = 0, \\
O(\varepsilon^2) &: M_\vartheta\binom{w_2}{n_2} = -\binom{f_1^{(1)}}{f_2^{(1)}} \\
O(\varepsilon^3) &: M_\vartheta\binom{w_3}{n_3} = \frac{\partial}{\partial\kappa}\binom{w_1}{n_1} - M\binom{w_1}{n_1} - \binom{f_1^{(2)}}{f_2^{(2)}},
\end{aligned}
$$

where the linear system (3.3) can be expressed as follows

$$
U_t = \left[M_\vartheta + \upsilon^2 M\right]U,
$$

$$
M = \begin{pmatrix} \alpha_{11}^{(2)} + \gamma^{(2)}\triangle & \alpha_{12}^{(2)} - \gamma^{(2)}\beta\triangle \\ \alpha_{21}^{(2)} & \alpha_{22}^{(2)} \end{pmatrix}
$$

$$
M_\vartheta = \begin{pmatrix} \alpha_{11}^{TH} - \gamma^{TH}\vartheta^2 & \alpha_{12}^{TH} + \gamma^{TH}\beta\vartheta^2 \\ \alpha_{21}^{TH} & \alpha_{22}^{TH} - \vartheta^2 \end{pmatrix}
$$

$$
\binom{f_1^{(1)}}{f_2^{(1)}} = \binom{\alpha_1 w^2 + \alpha_2 wn + \alpha_3 n^2}{\beta_1 w^2 + \beta_2 wn + \beta_3 n^2}, \quad \binom{f_1^{(2)}}{f_2^{(2)}} = \binom{2\alpha_1 w_1 w_2 + \alpha_2(w_1 n_2 + w_2 n_1) + 2\alpha_3 n_1 n_2 + \alpha_4 w_1^3}{2\beta_1 w_1 w_2 + \beta_2(w_1 n_2 + w_2 n_1) + 2\beta_3 n_1 n_2 + \beta_4 w_1^3},
$$

and $\alpha_{ij}^{TH} = \alpha_{ij}\big|_{R=R_{0,H}, \gamma_T^*}$ $i, j = 1, 2$ and $\gamma^{TH} = \gamma_T^*$. Note that

$$
M_{\vartheta^*}q = 0, \quad M_0 q = i\omega_H p,
$$

which takes us to deduce that

$$
q = \binom{q_1}{q_2} = \binom{\frac{\alpha_{12}^{TH} + \beta\vartheta^2}{\vartheta^2 - \alpha_{11}^{TH}}}{1}, \quad p = \binom{p_1}{p_2} = \binom{\frac{\alpha_{12}^{TH} + \beta\vartheta^2}{i\omega_H - \alpha_{11}^{TH}}}{1}.
$$

Now we set

$$
\binom{w_1}{n_1} = \sum_{j=1}^{3}\binom{X_j}{\tilde{X}_j}\exp^{i\vartheta_j x} + \binom{\Phi_1}{\Phi_2}\exp^{i\omega_H t} + c.c.,
\tag{3.13}
$$

where $|\vartheta_j|^2 = \vartheta_T$, $j = 1, 2, 3$, This means that

$$
\binom{X_j}{\tilde{X}_j} = q\Lambda_j, \quad \binom{\Phi_1}{\Phi_2} = p\Phi.
$$

Based on the above results, we suppose that the type of solutions $U^{(2)}$ can be expressed in the following manner

$$
\binom{w_2}{n_2} = \binom{W_0}{N_0} + \sum_{j=1}^{m} \left[\binom{W_j}{N_j} \exp^{i\vartheta_j \cdot x} + \binom{W_{jj}}{N_{jj}} \exp^{i2\vartheta_j \cdot x} \right]
$$
$$
+ \binom{W_H}{N_H} \exp^{i2\omega_H \cdot t} + \sum_{n \neq j > 0} \binom{W_{nj}}{N_{nj}} \exp^{i(\vartheta_n - \vartheta_j) \cdot x} + \binom{W_{TH}}{N_{TH}} + c.c.
$$

(3.14)

By injecting the Eq. (3.14) into $O(\varepsilon^2)$ we get

$$
(\alpha_{11}^{TH} + \gamma\triangle)w_2 + (\alpha_{12}^{TH} - \beta\triangle)n_2 = -(\alpha_1 w_1^2 + \alpha_2 w_1 n_1 + \alpha_3 n_3^2),
$$
$$
\alpha_{21}^{TH} w_2 + (\alpha_{22}^{TH} + \triangle)n_2 = -(\beta_1 w_1^2 + \beta_2 w_1 n_1 + \beta_3 n_1^2).
$$

Then we can put

$$
W_0 = W_0^T + W_0^H, \quad W_0^T = \Theta_{1T} N_0^T, \quad N_0^T = \Theta_{2T}|P_j|^2, \quad W_0^H = \Theta_{1H} N_0^H,
$$
$$
N_0^H = \Theta_{2H}|\Phi|^2, \quad W_j = q_1 N_j, \quad W_{12} = \Theta_5 N_{12},
$$
$$
N_{jj} = \Theta_4 P_j^2, \quad N_{12} = \Theta_6 P_1 P_2, \quad W_H = \Theta_7 N_H, \ N_H = \Theta_8 \Phi^2,
$$
$$
W_{TH} = \Theta_9 N_{TH}, \quad N_{TH} = \Theta_{10} P_j \Phi, \quad W_{jj} = \Theta_3 N_{jj},
$$

such that

$$
\Theta_{1T} = \frac{\beta_T \alpha_{12}^{TH} \alpha_T \alpha_{22}^{TH}}{\alpha_T \alpha_{21}^{TH} - \beta_T \alpha_{11}^{TH}},
$$
$$
\Theta_{1H} = \frac{\beta_H \alpha_{12}^{TH} \alpha_H \alpha_{22}^{TH}}{\alpha_H \alpha_{21}^{TH} - \beta_H \alpha_{11}^{TH}}, \quad \Theta_{2T} = \frac{-\alpha_T}{\alpha_{11}^{TH}\Theta_{1T} + \alpha_{12}^{TH}},
$$
$$
\Theta_{2H} = \frac{-\alpha_H}{\alpha_{11}^{TH}\Theta_{1H} + \alpha_{12}^{TH}}, \quad \Theta_3 = \frac{\alpha_{2T}(\alpha_{22}^{TH} - 4\vartheta^2) - \beta_{2T}\alpha_{12}^{TH} + \beta\gamma^{TH}\vartheta^2}{\beta_{2T}(\alpha_{11}^{TH} - 4\gamma^{TH}\vartheta^2) - \alpha_{2T}\alpha_{21}^{TH}},
$$
$$
\Theta_4 = -\frac{-\alpha_{2T}}{(\alpha_{11}^{TH} - 4\vartheta^2)\Theta_3 + \alpha_{12}^{TH} + \beta\gamma^{TH}\vartheta^2},
$$
$$
\Theta_5 = \frac{\alpha_{3T}(\alpha_{22}^{TH} - 3\vartheta^2) - \beta_{3T}\alpha_{12}^{TH} + \beta\gamma^{TH}\vartheta^2}{\beta_{3T}(\alpha_{11}^{TH} - 3\gamma^{TH}\vartheta^2) - \alpha_{3T}\alpha_{21}^{TH}},
$$
$$
\Theta_6 = -\frac{-\alpha_{3T}}{(\alpha_{11}^{TH} - 3\vartheta^2)\Theta_5 + \alpha_{12}^{TH} + \beta\gamma^{TH}\vartheta^2},
$$
$$
\Theta_7 = \frac{\beta_{4H}\alpha_{12}^{TH}\alpha_{4H}\alpha_{22}^{TH}}{\alpha_{4H}\alpha_{21}^{TH} - \beta_{4H}\alpha_{11}^{TH}},
$$
$$
\Theta_8 = \frac{-\alpha_{4H}}{\alpha_{11}^{TH}\Theta_{1H} + \alpha_{12}^{TH}}, \quad \Theta_9 = \frac{\alpha_{5T}(\alpha_{22}^{TH} - \vartheta^2) - \beta_{5T}\alpha_{12}^{TH} + \beta\gamma^{TH}\vartheta^2}{\beta_{5T}(\alpha_{11}^{TH} - \gamma^{TH}\vartheta^2) - \alpha_{5T}\alpha_{21}^{TH}},
$$
$$
\Theta_{10} = -\frac{-\alpha_{5T}}{(\alpha_{11}^{TH} - 4\vartheta^2)\Theta_9 + \alpha_{12}^{TH} + \beta\gamma^{TH}\vartheta^2},
$$
$$
\alpha_T = 2\alpha_1|q_1|^2 + \alpha_2(q_1\overline{q}_2 + q_2\overline{q}_1) + 2\alpha_3|q_2|^2, \quad \beta_T = 2\beta_1|q_1|^2 + \beta_2(q_1\overline{q}_2 + q_2\overline{q}_1) + 2\beta_3|q_2|^2,
$$
$$
\alpha_H = 2\alpha_1|p_1|^2 + \alpha_2(p_1\overline{p}_2 + p_2\overline{p}_1) + 2\alpha_3|p_2|^2, \quad \beta_H = 2\beta_1|p_1|^2 + \beta_2(p_1\overline{p}_2 p_2\overline{p}_1) + 2\beta_3|p_2|^2,
$$
$$
\alpha_{2T} = \alpha_1 q_1^2 + \alpha_2 q_1 q_2 + \beta_3 q_2^2,
$$
$$
\beta_{2T} = \beta_1 q_1^2 + \beta_2 q_1 q_2 + \beta_3 q_2^2, \quad \alpha_{3T} = \alpha_T, \quad \beta_{3T} = \beta_T, \quad \alpha_{4H} = \alpha_{2T}, \quad \beta_{4H} = \beta_{2T},
$$
$$
\alpha_{5T} = 2\alpha_1 q_1\overline{p}_1 + \alpha_2(q_1\overline{p}_2 + q_2\overline{p}_1) + 2\alpha_3 q_2\overline{p}_2,
$$
$$
\beta_{5T} = 2\beta_1 q_1\overline{p}_1 + \beta_2(q_1\overline{p}_2 + q_2\overline{p}_1) + 2\beta_3 q_2\overline{p}_2.
$$

Now, we solve the system of $O(\varepsilon^3)$ term. Based on the condition of Fredholm Solubility [16]. The right-hand side of the mentioned equation has to be perpendicular to the zero eigenvectors of the adjoint operator M_ϑ^+. At first, the zero eigenvectors of M_ϑ^+ to the Turing bifurcation is $q^* \exp^{-\vartheta_j \cdot x}$ where $q^* = (q_1^*, q_2^*) = \left(1, \frac{\alpha_{11}^{TH} - \gamma\vartheta^2}{\alpha_{21}^{TH}}\right)^T$. Note that M_ϑ^+ is the conjugate of M_ϑ. Thus, the zero eigenvector of the operator M_ϑ^+ to the Hopf bifurcation is

$p^* \exp^{-\omega_H \cdot t}$ where $p^* = \left(p_1^*, p_2^*\right)^T = \left(1, \frac{\alpha_{11}^{TH}}{\alpha_{21}^{TH}}\right)^T$. The orthogonality condition offered by M_ϑ^+ with the third order term can e expressed as

$$(q_1^*, q_2^*) \exp^{-\vartheta_j r} M_\vartheta \binom{w_3}{n_3} = 0, \quad (p_1^*, p_2^*) \exp^{-i\omega_H t} M_\vartheta \binom{w_3}{n_3} = 0.$$

Then we get (by using the Fredholm solubility condition)

$$\tau_0 \frac{\partial P_1}{\partial \kappa} = \overline{\mu} P_1 + C(\overline{n_2 P_3} + \overline{n_3 P_2}) + \left(g_1'|P_1|^2 + g_2'(|P_2|^2 + |P_3|^2)\right) P_1 + g_3'|\Phi|^2 P_1,$$

such that $\tau_0, \overline{\mu}, C, g_1', g_2', g_3'$ are defined in "Appendix" section.

The equations of P_2 and P_3 could be obtained using the subscript change of P. Using the above expressions and

$$\begin{aligned}
A_j &= \binom{A_j^w}{A_j^n} = \binom{q_1}{q_2} \left(\varepsilon P_j + \varepsilon^2 P_j + O(\varepsilon^3)\right), \\
B_j &= \binom{B_j^w}{B_j^n} = \binom{p_1}{p_2}\varepsilon B, \\
\frac{\partial A_j^w}{\partial t} &= \varepsilon^3 q_1 \frac{\partial P_j}{\partial \kappa} + O(\varepsilon^4), \quad j = 1, 2, 3, \\
\frac{\partial B_j^w}{\partial t} &= \varepsilon^3 p_1 \frac{\partial B}{\partial \kappa} + O(\varepsilon^4),
\end{aligned}$$

then the amplitude equations at Turing mode (three equations) and Hopf bifurcation modes (one equation) with the orthogonal wave vector are expressed as follows (see also [15]):

$$\begin{aligned}
\frac{\partial A_1^w}{\partial t} &= \mu A_1^w + h\overline{A_2^w A_3^w} + \left(g_1|A_1^w|^2 + g_2\left(|A_2^w|^2 + |A_3^w|^2\right)\right) A_1^w + g_3|B^w|^2 A_1^w, \\
\frac{\partial A_2^w}{\partial t} &= \mu A_2^w + h\overline{A_3^w A_1^w} + \left(g_1|A_2^w|^2 + g_2\left(|A_1^w|^2 + |A_3^w|^2\right)\right) A_2^w + g_3|B^w|^2 A_2^w, \\
\frac{\partial A_3^w}{\partial t} &= \mu A_3^w + h\overline{A_1^w A_2^w} + \left(g_1|A_3^w|^2 + g_2\left(|A_1^w|^2 + |A_2^w|^2\right)\right) A_3^w + g_3|B^w|^2 A_3^w, \\
\frac{\partial B_1^w}{\partial t} &= \xi B^w + g_{01}|B^w|^2 H^w + g_{02}(|A_1^w|^2 + |A_2^w|^2 + |A_3^w|^2)B^w,
\end{aligned}$$
(3.15)

where $h, \mu, \xi, g_{01}, g_{02}, g_1, g_2, g_3$ are defined at the "Appendix" section. For the subject of determining the patterns selections, we need to analyze the existence and the stability of equilibrium points to the amplitude Eq. (3.15). In fact, each amplitude could be decomposed into its module as $\psi_j = |A_j^w|$, $\varrho = |B|$. By a straightforward calculation, we get

$$\begin{aligned}
\frac{\partial \psi_1}{\partial t} &= \mu \psi_1 + h\psi_2 \psi_3 \cos v + \left(g_1|\psi_1^2| + g_2|\psi_2^2| + g_3|\psi_3^2|\right) \psi_1 + g_3|B|^2 \psi_1, \\
\frac{\partial \psi_2}{\partial t} &= \mu \psi_2 + h\psi_1 \psi_3 \cos v + \left(g_1|\psi_2^2| + g_2|\psi_1^2| + g_3|\psi_3^2|\right) \psi_2 + g_3|B|^2 \psi_2, \\
\frac{\partial \psi_3}{\partial t} &= \mu \psi_1 + h\psi_1 \psi_2 \cos v + \left(g_1|\psi_3^2| + g_2|\psi_2^2| + g_3|\psi_1^2|\right) \psi_3 + g_3|B|^2 \psi_3, \\
\frac{\partial \varrho}{\partial t} &= -h \frac{\psi_1^2 \psi_2^2 + \psi_1^2 \psi_3^2 + \psi_2^2 \psi_3^2}{\psi_1 \psi_2 \psi_3} \sin v, \\
\frac{\partial B}{\partial t} &= \xi B + \Re(g_{01})|B|^2 B + \Re(g_{02})(|\psi_1|^2 + |\psi_2|^2 + |\psi_3|^2)B, \\
\triangle\omega &= \Im(g_{01})|B|^2 + \Im(g_{02})(|\psi_1|^2 + |\psi_2|^2 + |\psi_3|^2),
\end{aligned}$$
(3.16)

where $v = \sum_{j=1}^3 \arg(A_j^w)$ and $H^w = B \exp^{i\triangle\omega t}$. For $h > 0$ the solution $\varrho = 0$ of the fourth equation of (3.16) is stable, and the solution $\varrho = \pi$ is stable under the condition $h < 0$. The patterns exist only when the solution of the fourth equation of (3.16) is stable. Thus, the

mode equations have the following structure:

$$\frac{\partial \psi_1}{\partial t} = \mu \psi_1 + |h|\psi_2\psi_3 + \left(g_1|\psi_1^2| + g_2|\psi_2^2| + g_3|\psi_3^2|\right)\psi_1 + g_3|B|^2\psi_1,$$
$$\frac{\partial \psi_2}{\partial t} = \mu \psi_2 + |h|\psi_1\psi_3 + \left(g_1|\psi_2^2| + g_2|\psi_1^2| + g_3|\psi_3^2|\right)\psi_2 + g_3|B|^2\psi_2,$$
$$\frac{\partial \psi_3}{\partial t} = \mu \psi_1 + |h|\psi_1\psi_2 + \left(g_1|\psi_3^2| + g_2|\psi_2^2| + g_3|\psi_1^2|\right)\psi_3 + g_3|B|^2\psi_3,$$
$$\frac{\partial B}{\partial t} = \xi B + \Re(g_{01})|B|^2 B + \Re(g_{02})(|\psi_1|^2 + |\psi_2|^2 + |\psi_3|^2)B,$$

(3.17)

Case 1. The solution of spatiotemporal periodic patterns is investigated, this means that

$$\psi_1 = \sqrt{\frac{\xi g_3 - \mu\Re(g_{01})}{g_1\Re(g_{01}) - g_3\Re(g_{02})}}, \quad \psi_2 = \psi_3 = 0, \quad B = \sqrt{\frac{-\xi g_1 + \mu\Re(g_{02})}{g_1\Re(g_{01}) - g_3\Re(g_{02})}}.$$

For having the stability with respect to the mode ψ_1 and B the condition $g_1\Re(g_{01}) > g_3\Re(g_{02})$ is required. The condition at which the solution exists reduces to $\mu\Re(g_{02}) \geq \xi g_1$, $\xi g_3 \geq \mu\Re(g_{01})$.

Case 2. Considers $\psi_1 = \psi_2 = \psi_3 = \psi$, and

$$\psi = \frac{|h| + \sqrt{|h|^2 - 4\left(g_1 + 2g_2 - 3\frac{g_3\Re(g_{02})}{\Re(g_{01})}\right)\left(\mu - \frac{\xi g_3}{\Re(g_{01})}\right)}}{2\left(g_1 + 2g_2 - 3\frac{g_3\Re(g_{02})}{\Re(g_{01})}\right)}, \quad |B|^2 = \frac{\xi + 3\Re(g_{02})|\psi|^2}{\Re(g_{01})}.$$

In this case the hexagonal patterns arise. For ensuring there existence and stability, the following conditions must be hold

$$|h|^2 - 4\left(g_1 + 2g_2 - 3\frac{g_3\Re(g_{02})}{\Re(g_{01})}\right)\left(\mu - \frac{\xi g_3}{\Re(g_{01})}\right) > 0, \quad g_1 + 2g_2 > 3\frac{g_3\Re(g_{02})}{\Re(g_{01})},$$

$$\frac{\xi + 3\Re(g_{02})|\psi|^2}{\Re(g_{01})} > 0, \quad 2\Re(g_{01})|B|^2 + 3|h|\psi + 6(g_1 + 2g_2)\psi^2 < 0.$$

For returning back to the Turing bifurcation only it is sufficient to consider $B = 0$ where this case is investigated in many papers as it has been highlighted in the introduction section. For the Turing-Hopf bifurcation, the cases 1 and 2 show this spatiotemporal behavior (nonhomogeneous) generated by the presence of this type of co-dimensional bifurcation.

4 Numerical simulations

In this section, we will investigate the complex dynamics introduced by varying the rainfall and internal competition and the diffusion coefficient. Firstly, we discuss the method for choosing parameters based on real-world remarks. For the vegetation model (1.5), there exists a considerable interval of selecting the value of the model parameters. For instance, in the case of the rainfall constant, in our planet, there is a vast diversity in the quantity of the rainfall, which depends on the studied region, where the most significant value will be obtained in the tropic regions. In these areas, the quantity of the rainfall is very high, contrary to the desert regions, where the rain is very scarce, this gives us a very open choice of the rainfall rate for satisfying our theoretical applications. There is a quiet type of plants that can survive in a certain type of conditions of the scarcity of rain, we mention as example Opuntia ficus-indica, zebra cactus plant, golden barrel plant, and others. Besides, for the choice of the rate δ which represents the death rate of the plant which is affected by the type of plant, as
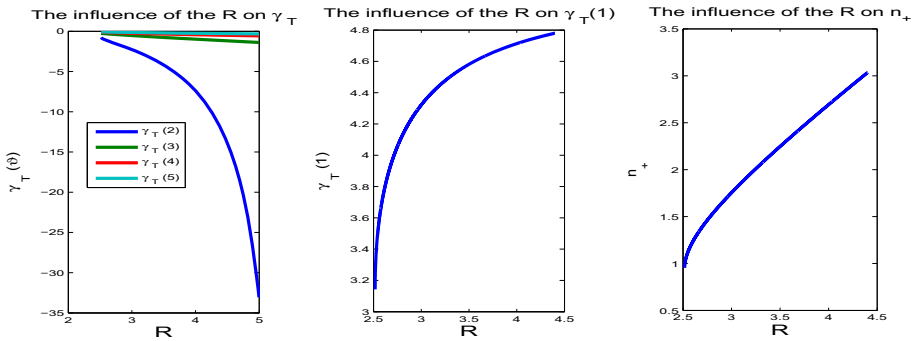
Fig. 1 The influence of the rainfall rate R on some critical parameters of the system (1.5)
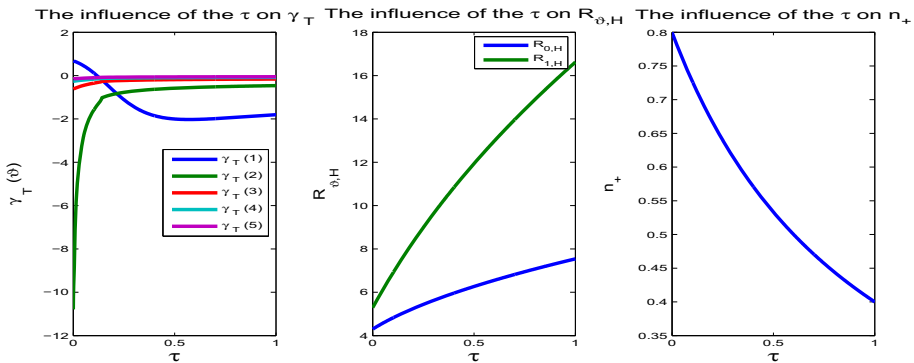

Fig. 2 The influence of the internal competition between plants τ on some critical parameters of the system (1.5)

for example, the death rate for a plant is very small for the trees, and some desert plants are very small compared to the grass (see [13]). For the plant's internal competition rate, there is also a wide interval that we can choose our parameters. In fact, this rate depends on the type of plants that can live in such as environment (where the type of environment is controlled by the rainfall constant) the reason for considering the kind of plant is due to the average of the consumed water by a plant, the length of the roots, the quantity of the consumed water by a plant (a type of the plant) and other factors which affect on determining the value of the internal competition rate. To mention that this last new parameter has been estimated in the numerical simulation. Also, the influence of this rate on the spatiotemporal dynamics is also established where it will be discussed later. In [13] it has been considered some value on the model (1.1) parameters that can be used here.

Fig. 1: Shows the impact of the rainfall rate on the positive homogenous steady state for the vegetation biomass n_+ and on the critical value of the Turing-Hopf bifurcation defined in (3.10). The following values are considered $\beta = 0.7$; $\delta = 1.2$; $\tau = 0.1$; $R_{min} = 2.5171$; $R_{0,H} = 3.5272$.

Fig. 2: Indicates the effect of the variable τ on positive homogenous steady state for the vegetation biomass n_+ and the impact on the critical value of the Turing-Hopf bifurcation defined in (3.10). The following values are taken: $\beta = 0.7$; $\delta = 2.2$; $R = 0.1$.
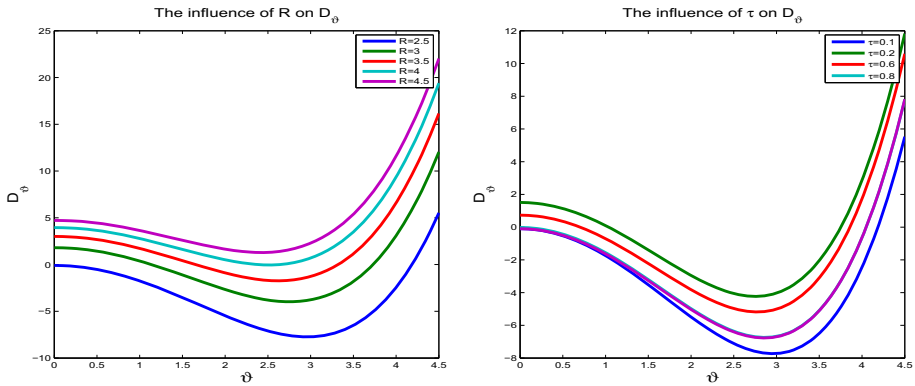
Fig. 3 The influence of the internal competition between plants τ on $D(\vartheta)$ Turing instability
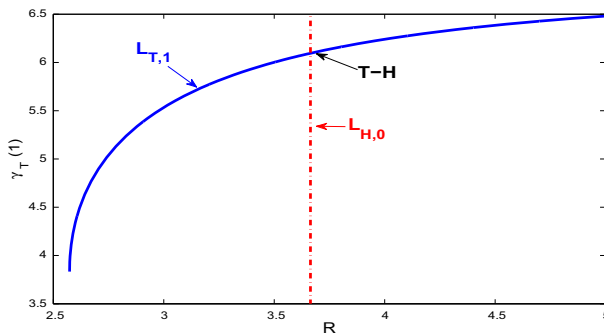

Fig. 4 The existence of Turing-Hopf bifurcation point which is the intersection point between the Hopf curve and Turing bifurcation curve denoted by $T - H$

Fig. 3: These figure shows that D_ϑ can be affected by the rainfall and the internal competition between plants, which means that it can affect the existence of Turing instability. The following values are chosen: $\gamma = 0.1$; $\beta = 0.7$; $\delta = 1.2$. In fact, for the left hand multi figure values of the rainfall next to $\tau = 0.15$ are considered, and the opposite is used for the right hand figure where the rainfall rate is fixed to the value $R = 3$, and multi values of the internal competition rate are used.

Fig. 4: This figure represents the existence of Turing-Hopf bifurcation point which is the intersection point between the Hopf bifurcation curve defined by $R = R_{0,H}$ (the figure in red) and Turing bifurcation curve $\gamma = \gamma_T(1)$ defined in (3.10). The following values are chosen: $\gamma = 0.1$; $\beta = 0.7$; $\delta = 1.2$; $\tau = 0.15$.

Fig. 5, 6: These figures show the influence of γ on the spatiotemporal behavior of the solution of the vegetation model (1.5) where $\beta = 0.7$; $\delta = 1.2$; $\tau = 0.6$; $R = 4.8 > R_{0,H}$.

Fig. 7, 8: These figures show the influence of γ on the spatiotemporal behavior of the solution of the vegetation model (1.5) where $\beta = 0.7$; $\delta = 1.2$; $\tau = 0.6$; $R = 4.7 < R_{0,H}$.
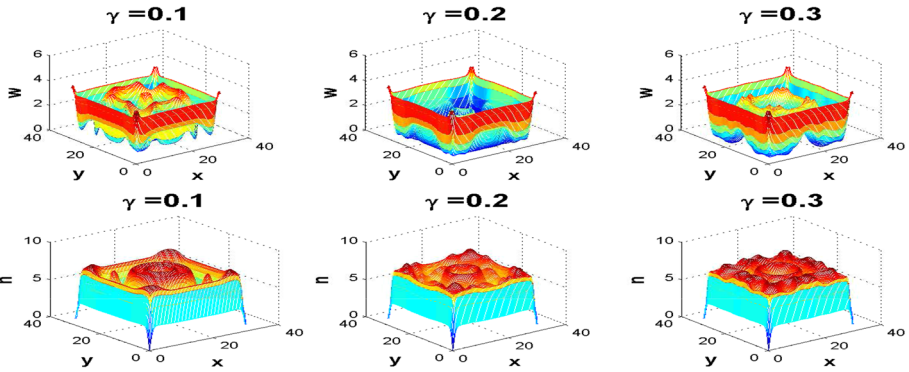
Fig. 5 the effect of γ on the spatiotemporal behavior under the initial conditions $(w_0(x, y), n_0(x, y)) = (0.1 + 0.01(\cos x + \cos y), 0.15 + 0.017(\cos x + \cos y))$

Fig. 6 The projection of the surfaces obtained in Fig. 5 on $x - y$ plan

Fig. 7 the effect of γ on the spatiotemporal behavior under the initial conditions $(w_0(x, y), n_0(x, y)) = (0.1 + 0.01(\cos x + \cos y), 0.15 + 0.017(\cos x + \cos y))$
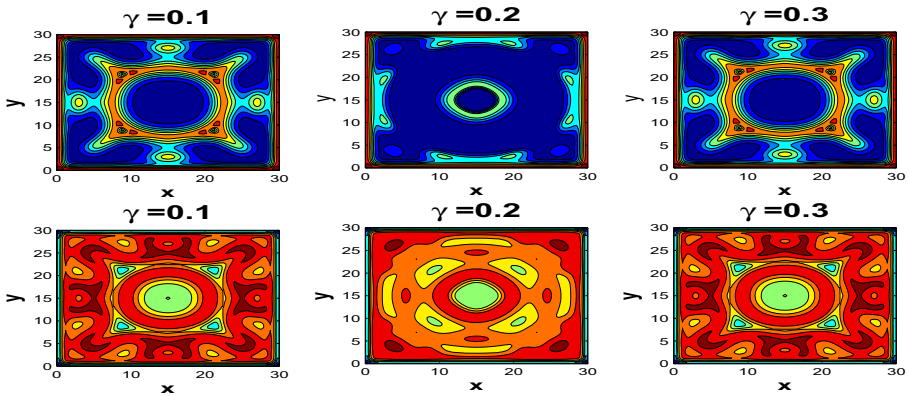
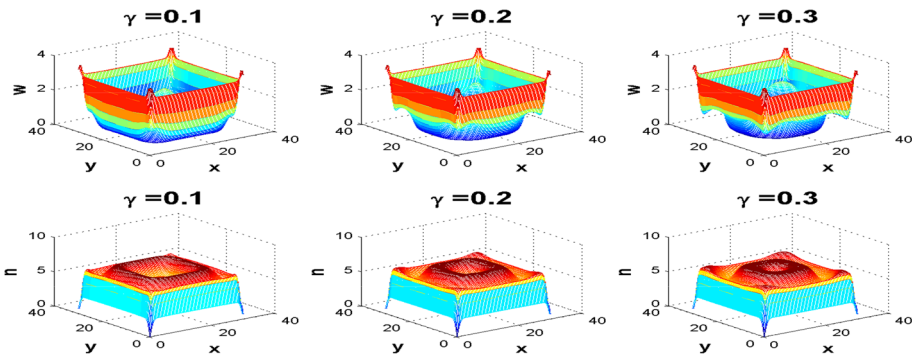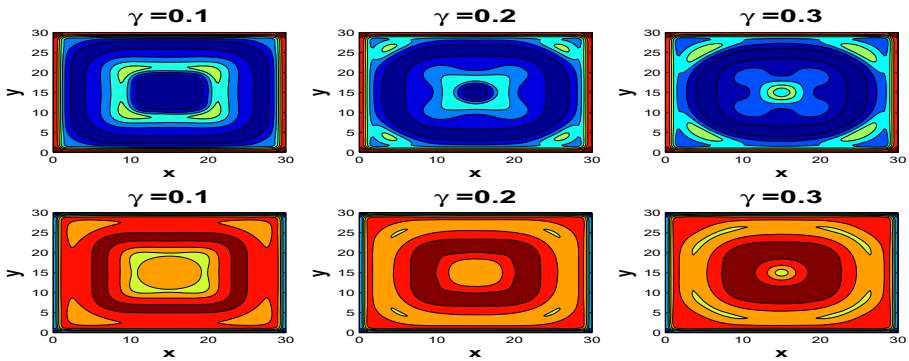**Fig. 8** The projection of the surfaces obtained in Fig. 7 on $x - y$ plan

5 Discussion and remarks

In this paper, we considered a predicting vegetation model by taking into account the water restriction by the plant's roots and the inner rivalry between the plants. Before we begin with our analysis, we recall that the inner competition between plants is just recently considered due to the paper [37], where it has been noticed that the model (1.3) cannot undergo Turing instability. Further, the main interest in the mentioned paper is to determine the patterns generated by the presence of the slope of the terrain next to the influence of internal rivalry between plants. Furthermore, there is no discussion on the types of bifurcation that the model can undergo. Based on existing works in the literature (vegetation patterns) such as the works [11,36] we can highlight that the patterns generated by the presence of Turing bifurcation is the most common for many papers. In this context, we achieved some new results for the vegetation results for determining vegetation patterns which are elaborated by the presence of Hopf bifurcation for the non-spatial model (Theorem 3.1) wherein the paper [37] the local stability is discussed only. Further, the spatial Hopf bifurcation has never been studied for the vegetation model wherein Theorem 3.2 discusses this result in detail. To highlight that proving the existence of Hopf bifurcation for a spatial model is very important for predicting the seasonality effect on vegetation growth. Turing bifurcation is recently investigated due to the paper [11] where it has been proved that the system (1.2) (in the absence of slop of terrain) undergoes Turing bifurcation and did an excellent job in discussing the patterns in the neighborhood of the Turing bifurcation point. The presence of this result means in the actual world the possibility of existence of the vegetation cover with non equal distribution in the space, and this result is the most common in the real-world. To mention that the model studied by [11] is a particular case of our system (1.5). Turing bifurcation it self generates an important and complex patterns, which highlight the non homogeneous distribution of species, where it is applied in different disciplines, where for more information we refer to the readers to check the papers [47–49] The study is not confined to prove the existence of these two types of bifurcations (Hopf bifurcation and Turing bifurcation), but it is expanded to show the possibility of the intermingling of both Turing and Hopf bifurcations for different wavenumbers (0 and ϑ_T). It is proved that Turing-Hopf bifurcation generates very complex dynamics in the case of predator-prey models [4,9,14,29], mussel-algae model [30], but has never been applied to vegetation model, and no one can deny its importance. Further, the existence of Turing-Hopf bifurcation in the case

of two-dimensional space is a very new step where some new arguments are provided for determining this kind of bifurcation.

Indeed, we investigated the influence of the type of climate measured by the rainfall constant R on the spatial patterns wherein Fig. 1 shows this result. More precisely, for the left-hand figure, it shows that γ_T defined in (3.10) is decreasing in R for different values of the wavenumber $\vartheta \neq 1, 0$ and increasing for $\vartheta = 1$ (the figure in the middle) which shows the significant influence of these rates on the critical value of the Turing-Hopf bifurcation. Further, it has been noticed that the rainfall has a positive impact on the vegetation equilibrium state n_+ as it has been shown in the left-hand of Fig. 1 which agrees with the real-life situations. In Fig. 2, the influence of the internal competition between plants on the critical values that we obtained in our analysis, as γ_T for different wave numbers $\vartheta \neq 0$ in the left-hand figure where a varying impact has been remarked on the critical value of Turing instability γ_T and positive impact on Hopf bifurcation (the figure in the middle), and negative impact on the vegetation equilibrium state n_+ which agrees with the real-world situation (by increasing the competition between the plants the vegetation density decreases). Furthermore, this influence (R and τ) has been expanded to Turing instability in Fig. 3, which allow us to claim that these two parameters influenced Turing patterns, and this shows the importance of considering the internal competition between plants on the vegetation model. Based on the obtained figures in Figs. 5, 6, 7, and 8, we can claim the complex dynamics generated by the presence of the water redistribution by the plant's roots next to the internal competition between plants, which is very important in predicting vegetation patterns.

As one of the results obtained in this study, we can mention that the spatial Hopf bifurcation achieved in the Theorem 3.2 is very essential for portending the vegetation patterns which can explain the seasonality of the vegetation in the case of the stable periodic solutions generated by the presence of Hopf bifurcation. The Turing bifurcation is also investigated where the influence of the water distribution in the soil by the roots next to the internal competition between plants is investigated in detail which is the main objective of our study. The presence of Hopf bifurcation can represent the impact of seasonality of the vegetation growth, wherein the actual world, we can remark that there are some seasons with a low density of the vegetation cover (for instance summer season), where the water is scarce, and there are other seasons with a high density of vegetation (for instance example the spring) where we can get a high density of vegetation cover. Furthermore, The intermingling between the Hopf and Turing bifurcation is also established for different wave numbers which are known by Turing-Hopf bifurcation, where an important agreement between the mathematical and the observation is noticed. In the actual world, it can present the possibility of having the seasonality effect generated by the presence of Hopf bifurcation and the nonhomogeneous distribution generated by the presence of Turing bifurcation. These results show the agreement between the mathematical findings and ecological observations.

Data Availability Statement Data sharing is not applicable to this article as no new data were created or analyzed in this study.

Appendix

$$\tau_0 = q_1 q_1^* + q_2 q_2^*, \quad \overline{\mu} = q_1 q_1^* \left(\alpha_{11}^{(2)} + \gamma^{(2)} \vartheta^2\right) + q_1 q_2^* \alpha_{21}^{(2)}$$
$$+ q_2 q_1^* \left(\alpha_{12}^{(2)} - \gamma^{(2)} \beta \vartheta^2\right) + q_2 q_2^* \alpha_{22}^{(2)},$$
$$C = q_1^* (2\alpha_1 q_1^2 + \alpha_2 q_1 q_2 + 2\alpha_3 q_2^2) + q_2^* (2\beta_1 q_1^2 + \beta_2 q_1 q_2 + 2\beta_3 q_2^2),$$
$$g_1' = (\Theta_{1T}\Theta_{2T} + \Theta_3\Theta_4)\left(q_1^*(2\alpha_1 q_1 + \alpha_2 q_2) + q_2^*(2\beta_1 q_1 + \beta_2 q_2)\right)$$
$$+ (\Theta_{2T} + \Theta_4)\left(q_1^*(\alpha_2 q_1 + 2\alpha_3 q_2) + q_2^*(\beta_2 q_1 + 2\beta_3 q_2)\right) + 3\alpha_4 q_1^3,$$
$$g_2' = (\Theta_{1T}\Theta_{2T} + \Theta_3\Theta_4)\left(q_1^*(2\alpha_1 q_1 + \alpha_2 q_2) + q_2^*(2\beta_1 q_1 + \beta_2 q_2)\right)$$
$$+ (\Theta_{2T} + \Theta_6)\left(q_1^*(\alpha_2 q_1 + 2\alpha_3 q_2) + q_2^*(\beta_2 q_1 + 2\beta_3 q_2)\right) + 6\alpha_4 q_1^3,$$
$$g_3' = \Theta_{1H}\Theta_{2H}\left(2q_1^*(\alpha_1 q_1 + \alpha_3 q_2) + 2q_2^*(\beta_1 q_1 + \beta_3 q_2)\right)$$
$$+ \Theta_{2H}(q_1 + q_2)\left(q_1^*\alpha_2 + q_2^*\beta_2\right) + 6(q_1^*\alpha_4 + q_2^*\beta_4)q_1|p_1|^2.$$
$$h = \frac{C}{\tau_0 q_1}, \quad g_1 = \frac{g_1'}{\tau_0 q_1^2}, \quad g_2 = \frac{g_2'}{\tau_0 q_1^2}, \quad g_3 = \frac{g_3'}{\tau_0 p_1^2},$$
$$\xi = \frac{q_1 p_2^2 (R - R_{H,0})\alpha_{21}^{(1)}}{q_1 p_1^* + q_2 p_2^*},$$
$$\mu = q_1 q_1^* \left(\alpha_{11}^{(1)}(R - R_{H,0}) + (\gamma - \gamma_T^*)\vartheta^2\right) + q_1 q_2^* \alpha_{21}^{(1)}(R - R_{H,0})$$
$$+ q_2 q_1^* \left(\alpha_{12}^{(1)}(R - R_{H,0}) - (\gamma - \gamma_T^*)\beta \vartheta^2\right) + q_2 q_2^* \alpha_{22}^{(1)},$$
$$g_{01} = \frac{1}{(q_1 p_1^* + q_2 p_2^*)q_1^2} \left(p_1^* \left((2\alpha_1 \overline{p}_1 + \alpha_2 \overline{p}_2)\Theta_7\Theta_8 \right. \right.$$
$$+ (\alpha_2 \overline{p}_1 + 2\alpha_3 \overline{p}_2)\Theta_8 + 3\alpha_4|p_1|^2 p_1 \right)$$
$$+ p_2^2 \left((2\beta_1 \overline{p}_1 + \beta_2 \overline{p}_2)\Theta_7\Theta_8 \right.$$
$$\left. \left. + (\beta_2 \overline{p}_1 + 2\beta_3 \overline{p}_2)\Theta_8 + 3\beta_4|p_1|^2 p_1 \right) \right),$$
$$g_{02} = \frac{1}{(q_1 p_1^* + q_2 p_2^*)q_1^2} \left(p_1^* \left((2\alpha_1 \overline{q}_1 + \alpha_2 \overline{q}_2)\Theta_9\Theta_{10} + (\alpha_2 \overline{q}_1 + 2\alpha_3 \overline{q}_2)\Theta_{10} + 3\alpha_4|q_1|^2 p_1 \right) \right.$$
$$+ p_2^2 \left((2\beta_1 \overline{q}_1 \right.$$
$$\left. \left. + \beta_2 \overline{q}_2)\Theta_9\Theta_{10} + (\beta_2 \overline{q}_1 + 2\beta_3 \overline{q}_2)\Theta_{10} + 3\beta_4|q_1|^2 p_1 \right) \right),$$

References

1. H. Amann, Dynamics theory of quasilinear parabolic equation. I. Abstract evolution equation, Nonlinear Anal. 12, 219–250 (1997)
2. B. Adams, J. Carr, Spatial pattern formation in a model of vegetation-climate feedback. Nonlinearity **16**(4), 13–39 (2003)
3. N. Barbier, P. Couteron, J. Lejoly, V. Deblauwe, O. Lejeune, Self-organized vegetation patterning as a fingerprint of climate and human impact on semiarid ecosystems. J. Ecol. **94**(3), 537–547 (2006)
4. I. Boudjema, S. Djilali, Turing-Hopf bifurcation in Gauss-type model with cross-diffusion and its application. Nonlinear Stud. **25**(3), 665–687 (2018)
5. F. Borgogno, P. D'Odorico, F. Laio, L. Ridolfi, Mathematical models of vegetation pattern formation in ecohydrology. Rev. Geophys. **47**, 1–36 (2009)
6. M.C. Cross, P.C. Hohenberg, Pattern formation outside of equilibrium. Rev. Mod. Phys. **65**(3), 851 (1993)
7. S. Djilali, Impact of prey herd shape on the predator-prey interaction. Chaos Solitons Fract. **120**, 139–148 (2019)
8. S. Djilali, S. Bentout, Spatiotemporal patterns in a diffusive predator-prey model with prey social behavior. Acta Applicandae Mathematicae. **169**, 125–143 (2020)
9. S. Djilali, Pattern formation of a diffusive predator-prey model with herd behavior and nonlocal prey competition. Math. Meth. Appl. Scien. **43**(5), 2233–2250 (2020)
10. K. Gowda, H. Riecke, M. Silber, Transitions between patterned states in vegetation models for semiarid ecosystems. Phys. Rev. E **89**, 022701 (2014)
11. G.Q. Sun, C.H. Wang, L.L. Chang, Y.P. Wu, L. Li, Effects of feedback regulation on vegetation patterns in semi-arid environments. Appl. Math. Model. **61**, 200–215 (2018)

12. R. HillerisLambers, M.G. Rietkerk, F. van den Bosch, H. Prins, H. Kroon, Vegetation pattern formation in semi-arid grazing systems. Ecology **82**, 50–61 (2001)
13. C.A. Klausmeier, Regular and irregular patterns in semiarid vegetation. Science **284**, 1826–1828 (1999)
14. X. Liu, T. Zhang, X. Meng, T. Zhang, Turing-Hopf bifurcations in a predator-prey model with herd behavior, quadratic mortality and prey-taxis. Phys. A **496**, 446–460 (2018)
15. B. Liu, R. Wu, L. Chen, Turing-Hopf bifurcation analysis in a superdiffusive predator-prey model. Chaos **28**, 113118 (2018)
16. N.I. Muskhelishvili, *Singular Integral Equations?: Boundary Problems of Function Theory and Their Application to Mathematical Physics* (Dover Publications, New York, 2013)
17. A. Pazy, *Semi Groups of Liner Operators and Applications to Partial Differential Equations* (Springer, Berlin, 2012)
18. J.A. Sherratt, Pattern solutions of the Klausmeier model for banded vegetation in semiarid environments IV: slowly moving patterns and their stability. SIAM, J. Appl. Math. **73**, 330–350 (2013)
19. J.A. Sherratt, G.J. Lord, Nonlinear dynamics and pattern bifurcations in a model for vegetation stripes in semi-arid environments. Theor. Popul. Biol. **71**, 1–11 (2007)
20. J.A. Sherratt, Pattern solutions of the Klausmeier model for banded vegetation in semi-arid environments II: patterns with the largest possible propagation speeds. Proc. R. Soc. A **467**, 3272–3294 (2011)
21. J.A. Sherratt, Pattern solutions of the Klausmeier model for banded vegetation in semi-arid environments III: the transition between homoclinic solutions. Physica D **242**, 30–41 (2013)
22. S. Djilali, B. Ghanbari, The influence of an infectious disease on a prey-predator model equipped with a fractional-order derivative. Adv. Differ. Equ. (2021). https://doi.org/10.1186/s13662-020-03177-9
23. F. Souna, A. Lakmeche, S. Djilali, Spatiotemporal patterns in a diffusive predator-prey model with protection zone and predator harvesting. Chaos Solitons Fract. **140**, 110180 (2020)
24. S. Djilali, Spatiotemporal patterns induced by cross-diffusion in predator-prey model with prey herd shape effect. Int. J. Biomath. **13**(4), 2050030 (2020). https://doi.org/10.1142/S1793524520500308
25. S. Bentout, Y. Chen, S. Djilali, Global dynamics of an SEIR model with two age structures and a nonlinear incidence. Acta Appl. Math. (2021). https://doi.org/10.1007/s10440-020-00369-z
26. S. Bentout, S. Djilali, B. Ghanbari, Backward, Hopf bifurcation in a heroin epidemic model with treat age. Int. J. Modeling Simul. Sci. Comput. (2020). https://doi.org/10.1142/S1793962321500185
27. G. Sun, L. Li, Z. Zhang, Spatial dynamics of a vegetation model in an arid flat environment. Nonlinear Dyn. **73**, 2207–2219 (2013)
28. F. Souna, S. Djilali, F. Charif, Mathematical analysis of a diffusive predator-prey model with herd behavior and prey escaping. Math. Model. Natural Phenom. (2018). https://doi.org/10.1051/mmnp/2019044
29. Y. Song, T. Zhang, Y. Peng, Turing-Hopf bifurcation in the reaction-diffusion equations and its applications. Commun. Nonlinear Sci. Numer. Simul. **33**, 229–258 (2016)
30. Y. Song, H. Jiang, Q.X. Liu, Y. Yuan, Spatiotemporal dynamics of the diffusive Mussel-Algae model near Turing-Hopf bifurcation. SIAM J. Appl. Dyn. Syst. **16**(4), 2030–2062 (2017)
31. X. Tang, Y. Song, T. Zhang, Turing-Hopf bifurcation analysis of a predator-prey model with herd behavior and cross-diffusion. Nonlinear Dyn. **86**(1), 73–89 (2016)
32. A.M. Turing, Philos. Trans. R. Soc. Lond. Ser. B Biol. Sci. **237**, 37–72 (1952)
33. C. Valentin, J.M. d'Herbes, J. Poesen, Soil and water components of banded vegetation patterns. Catena **37**, 1–24 (1999)
34. S. van der Stelt, A. Doelman, G.M. Hek, J. Rademacher, Rise and fall of periodic patterns for a generalized Klausmeier-gray-scott model. J. Nonlinear Sci. **23**, 39–65 (2012)
35. J. Von Hardenberg, E. Meron, M. Shachak, Y. Zarmi, Diversity of vegetation patterns and desertification. Phys. Rev. Lett. **87**, 198101 (2001)
36. X. Wang, W. Wang, G. Zhang, Vegetation pattern formation of a water-biomass model. Commun. Nonlinear Sci. Numer. Simulat. **42**, 571–584 (2017)
37. X. Wang, G. Zhang, Vegetation pattern formation in seminal systems due to internal competition reaction between plants. J. Theoret. Biol. **458**, 10–14 (2018)
38. T. Kuniya, T.M. Touaoula, Global stability for a class of functional differential equations with distributed delay and non-monotone bistable nonlinearity. Math. Biosci. Eng. **17**(6), 7332–7352 (2020)
39. T.M. Touaoula, Global dynamics for a class of reaction-diffusion equations with distributed delay and neumann condition. Commun. Pure Appl. Anal. **19**(5), 2473–2490 (2018)
40. M.N. Frioui, T.M. Touaoula, B.E. Ainseba, Global dynamics of an age-structured model with relapse. Discrete Contin. Dyn. Syst. Ser. B **25**(6), 2245–2270 (2020)
41. N. Bessonov, G. Bocharov, T.M. Touaoula, S. Trofimchuk, V. Volpert, Delay reaction-diffusion equation for infection dynamics. Discrete Contin. Dyn. Syst. Ser. B **24**(5), 2073–2091 (2019)
42. T.M. Touaoula, Global stability for a class of functional differential equations (Application to Nicholson's blowflies and Mackey-Glass models). Discrete Contin. Dyn. Syst. **38**(9), 4391–4419 (2018)

43. T.M. Touaoula, M.N. Frioui, N. Bessonov, V. Volpert, Dynamics of solutions of a reaction-diffusion equation with delayed inhibition. Discrete Contin. Dyn. Syst.-S **13**(9), 2425–2442 (2018)
44. M.N. Frioui, S.E.H. Miri, T.M. Touaoula, Unified Lyapunov functional for an age-structured virus model with very general nonlinear infection response. J. Appl. Math. Comput. **58**(5–6), 47–73 (2017)
45. P. Michel, T.M. Touaoula, Asymptotic behavior for a class of the renewal nonlinear equation with diffusion. Math. Methods Appl. Sci. **36**(3), 323–335 (2013)
46. I. Boudjema, T.M. Touaoula, Global stability of an infection and vaccination age-structured model with general nonlinear incidence. J. Nonlinear Funct. Anal. **2018**(33), 1–21 (2018)
47. M. Banerjee, S. Banerjee, Turing instabilities and spatio-temporal chaos in ratio-dependent Holling-Tanner model. Math. Biosci. **236**(1), 64–76 (2012)
48. M. Banerjee, S. Ghorai, N. Mukherjee, Study of cross-diffusion induced Turing patterns in a ratio-dependent prey-predator model via amplitude equations. Appl. Math. Model. **55**, 383–399 (2018)
49. M. Banerjee, Turing and non-turing patterns in two-dimensional prey-predator models. In: Banerjee S., Rondoni L. (eds) Applications of Chaos and nonlinear dynamics in science and engineering - Vol. 4 (2015) Understanding complex systems. Springer, Cham. https://doi.org/10.1007/978-3-319-17037-4_8